Half-fringe Photoelasticity: A New Approach to Whole-field Stress Analysis

by A.S. Voloshin and C.P. Burger

ABSTRACT—This paper presents a new method for whole-field stress analysis based on a symbiosis of two techniques—classical photoelasticity and modern digital image analysis. The resulting method is called 'half-fringe photoelasticity (HFP).'

Classical photoelasticity demands materials with high birefringence, which leads to extensive use of plastics as model materials. Since the behavior of these materials is often different from that of the prototype materials, their use distorts the similitude relationships. In many contemporary problems this distortion is untenable. HFP offers a way out of this dilemma. It permits materials and loads to be chosen so that no more than one half of a fringe order appears in the area of interest. Thus, for example, glass, which behaves linearly up to high stress levels and over a wide range of temperatures, could be used as model material. Alternatively, models from polymeric materials could be used under very low load in order to stay within the linear part of the stress-strain diagram and to prevent large deformations. The half-fringe-photoelasticity system, which is described here, utilizes the resulting low levels of birefringence for effective stress analysis.

This paper describes the system. It outlines a calibration routine and illustrates its application to two simple problems using glass models.

List of Symbols

A = constant
C = stress-optic coefficient
c = the relative stress-optic coefficient
f_σ = material fringe value
h = thickness of the specimen in the direction of light propagation
I = image brightness
K = constant
N = relative retardation in terms of complete cycles (fringe order)
Z = digital-output value
γ = slope of the scanner sensitivity curve
Δ = relative retardation in radians
λ = wavelength of the light
σ_i = in-plane principal stresses
ψ = constant

Introduction

Experimental studies which utilize stress- or strain-induced birefringence in transparent models of prototype structures have long been a powerful tool in our quest for more reliable structures. In the late 19th and early 20th centuries, researchers worked with models that were predominantly made of glass. After World War II the new polymeric materials, notably the epoxies, made possible better castability, machineability, and much higher stress-optical sensitivity. Thus, they took over as the preferred material for photoelastic models. These materials were adequate for the linear-elastic problems of the day, but with advancing technology new problems arose where the more traditional polymers were unable to correctly model prototype behavior. The standard similitude relations became distorted, and serious questions arose about the validity of translating photoelastic data to prototype behavior. This is particularly true in thermoelastic and thermoplastic problems, in plasticity studies, and in the areas of fracture mechanics and creep where nonlinear behavior occurs at discontinuities. Serious difficulties also arose in trying to formulate acceptable models for composite materials. In the stress freezing of complicated structures, the low moduli of the materials and the consequent large deformations of the models caused distortions in the similitude relationships. Also the problem of mismatching between the different Poisson ratios of model and prototype in multiply-connected problems was almost insurmountable.

At the same time that these modeling difficulties became evident, the electronic revolution tempted several researchers to incorporate automation into their polariscopes.[1-3] However, the integration between contemporary digital-computer technology and photoelasticity remained incomplete. This paper describes a complete system which fully integrates these two technologies. In addition to the vastly improved capabilities for data acquisition and the potential for complete automation of the process, the technique permits operating with low levels of birefringence. This opens the field to many model materials with otherwise desirable properties but low birefringence. Alternatively, traditional models may be used under much lower loads. This reduces the danger of nonlinear behavior in regions with steep stress gradients, reduces deformations during stress freezing, and generally simplifies the design of loading fixtures.

In principle, the technique, which we call half-fringe photoelasticity (HFP), brings together on-line digital image-processing procedures with photoelasticity. It is based on a digital gray-level analyzer and picture-processing system which divides its field of view into 640 by 480 picture elements and then assigns to each element its correct 'gray level' to an 8-bit resolution, i.e., within 256 gray levels. Thus, the intensity field of a half-fringe light-field photoelastic pattern can be divided into 256 levels from 'light' to 'dark,' for an equivalent theoretical fringe multiplication of 512 times. In practice, much lower levels of resolution are adequate. Once the programming procedures are established whereby the intensity field can be

A.S. Voloshin (SESA Member) and C.P. Burger (SESA Member) are Assistant Professor and Professor, respectively, Department of Engineering Science and Mechanics and Engineering Research Institute, Iowa State University, Ames, IA 50011.

Original manuscript submitted: February 3, 1983. Final version received: April 27, 1983.

converted into 'fringes' and hence to stresses, the system becomes fully automatic and its resolution is limited only by the extent to which the programming can filter out the optical 'noise' of any particular polariscope system.

Description of the System

The components of the half-fringe-photoelasticity system are diagrammed in Fig. 1. The system consists of a regular polariscope in which the camera or viewing lens is replaced with a video camera.[4] From this point on the system includes:

—an 'EYECOM' scanner which uses a special vidicon television-camera tube to scan the chosen image area. The picture is divided into 480 lines and each line is divided into 640 parts. The brightness (Z value) is converted into a video signal with 8-bit resolution. This division represents 307,200 points or picture elements (called 'pixels'). The intensity for each pixel is read and digitized on a scale which divides the range from a preselected darkest to a lightest point into 256 different gray levels.

—A real-time digitizer which digitizes the video signal in 1/30 second. This is too fast for direct transfer to the computer, so a special digitizer data bus transfers the data to the refresh memory where it can be accessed later by the computer.

—A display system or monitor which visualizes the information and acts as a graphics/numeric terminal for data processing, program development, and graphical data displays.

—A LSI-11/2 computer and peripherals.

Data Analysis

The stress-optic law for linear-elastic stress birefringence is:[4,5]

$$\Delta = \frac{2\pi hc}{\lambda}(\sigma_1 - \sigma_2) = C(\sigma_1 - \sigma_2)h \qquad (1a)$$

where

Δ = relative retardation, i.e., relative angular phase shift

σ_1 and σ_2 = in-plane principal stresses

c = the relative stress-optic coefficient in brewsters (1 brewster = $10^{-12}\text{m}^2/N$ = 6.9×10^{-9} in.^{2}/lb)

h = thickness of photoelastic slice in a direction normal to the σ_1, σ_2 plane, i.e., in the direction of propagation of the light

λ = wavelength of the light

$C = \frac{2\pi c}{\lambda}$ = stress-optic coefficient

For practical use, eq (1a) is reduced to

$$(\sigma_1 - \sigma_2) = \frac{Nf_\sigma}{h} \qquad (1b)$$

where

$N = \Delta/2\pi$ = relative retardation in terms of complete cycles of retardation

$f_\sigma = \frac{\lambda}{c} = \frac{2\pi}{C}$ N/m or lb/in. material fringe value or 'photoelastic-fringe constant.'

In a circular polariscope (dark field setup) the intensity of the transmitted light emerging from the analyzer is

$$I = K \sin^2 \frac{\Delta}{2} \qquad (2a)$$

where

K = a constant

Δ = the phase difference introduced between the two components of the light vector by the difference $(\sigma_1 - \sigma_2)$ of the principal stresses

The intensity $I = 0$ when $\Delta/2 = n\pi$ for $n = 0,1,2,3,\ldots$. For these values $N = \Delta/2\pi$ is always an integer, i.e., full-order fringe.

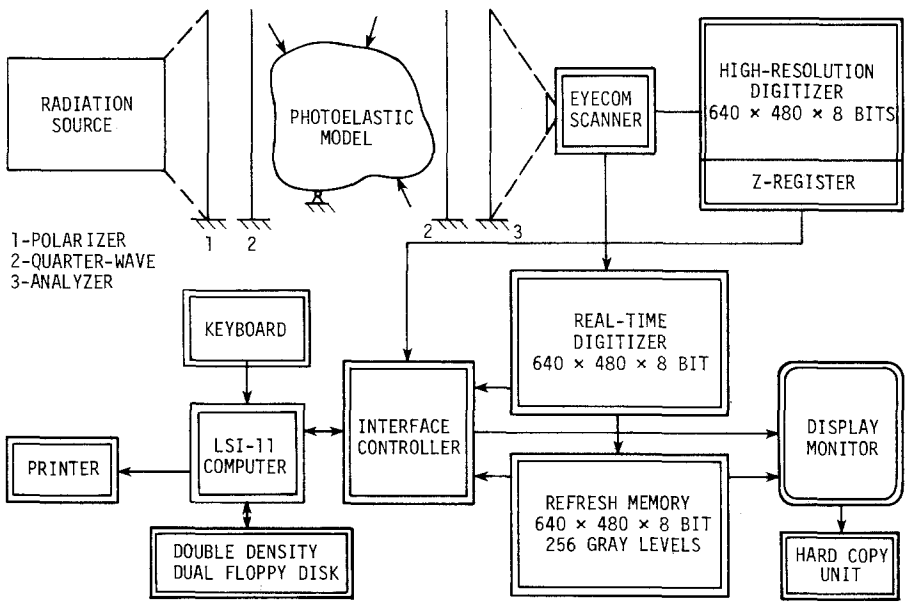

Fig. 1—Diagram of the HFP system

In the light-field setup for a circular polariscope the intensity is

$$I = K \cos^2 \frac{\Delta}{2} \tag{2b}$$

Extinction occurs when $I = 0$, i.e., when $\frac{\Delta}{2} = \frac{1+2n}{2}\pi$ for $n = 0, 1, 2, \ldots, n$. Then

$$N = \frac{\Delta}{2\pi} = 1/2 + n = 1/2, 3/2, 5/2, \ldots, (2n-1)/2$$

These are often called 'half-order' fringes. The light-intensity distribution for eq (2a) is shown in Fig. 2.

In half-fringe photoelasticity (HFP) the image-analysis system distinguishes between 256 gray levels in any interval from 0 to $\pi/2$, $\pi/2$ to π, and so on. If only one observation with a single frequency of monochromatic light is used, it cannot identify the interval; i.e., it cannot identify which half fringe it is reading. The experimental parameters in eqs (1a) or (1b) must, therefore, be chosen so that $0 < \Delta/2 < \pi/2$; i.e., $0 < N < ½$.

The digitization of the intensity plot in Fig. 2 occurs on the I axis so that equal gray-level divisions represent uneven stress increments. The correction for this sine-square relationship between intensity and partial 'fringe order' must be made in the data-interpretation programs of the HFP system.

In order to keep $N = h/f_\sigma(\sigma_1 - \sigma_2) < ½$, the parameters h, f_σ, and $(\sigma_1 - \sigma_2)$ must be selected accordingly. This requires that one or all of the following be true:

—low $(\sigma_1 - \sigma_2)$, i.e., low shear stresses in the models; this usually means that the model loads will be low;

—high f_σ, i.e., low-stress birefringence in the model material; and

—small h, i.e., thin models.

The first and last requirements are desirable in all photoelastic work. Low loads mean small deformations, reduced nonlinearity, and better modeling of prototype response. Thin models approximate plane stress better and/or make it easier to meet the requirement that the $(\sigma_1 - \sigma_2)$ field should not vary through the thickness of the model or slice. High f_σ (i.e., lower sensitivity to loads) has generally been abandoned by photoelasticians as an undesirable characteristic. With insensitive materials, high fringe order can only be obtained by using high loads and thick models. The drive for low values of f_σ has precluded the use of many model materials with otherwise highly desirable properties. For HFP, a high f_σ is often desirable since one must guard against having a fringe order that is too high. In general, these materials also have very low levels of residual birefringence—a distinct advantage in HFP.

Calibration Technique

The response of the vidicon tube, used in the video camera, is not linear with intensity. The Z value, or brightness recorded by the camera on a digital scale from 0 to 255, is related to the brightness I of the image through

$$Z = \psi I^\gamma \tag{3}$$

where

ψ = proportionality constant
γ = slope of the vidicon sensitivity line on a log I vs. log Z plot

To calibrate the system for photoelasticity, a reference intensity I_0 is introduced. Equation (2a) is rewritten to incorporate this reference intensity for a particular model/polariscope combination.

$$I = I_0 \sin^2 \frac{\Delta}{2} \tag{4a}$$

or

$$\frac{\Delta}{2} = \text{arc sin} \sqrt{\frac{I}{I_0}} \tag{4b}$$

Then from eq (1a)

$$(\sigma_1 - \sigma_2) = \frac{\Delta}{Ch} = \frac{2}{Ch} \text{arc sin} \sqrt{\frac{I}{I_0}} \tag{5}$$

where

I = the experimentally measured light intensity

Since the image-analysis system described here is able to measure light intensity I to a high degree of resolution, all that is necessary to convert it into a high-resolution stress-measurement system is a calibration procedure to link the output (Z) to the difference between the principal stresses $(\sigma_1 - \sigma_2)$. To illustrate the procedure, the calibration is here performed on a beam in pure bending (four-point loading).

The beam is loaded until the maximum fringe orders at the boundaries are in excess of 0.5 (Fig. 3). From the live image on the video screen, a transverse line is selected and

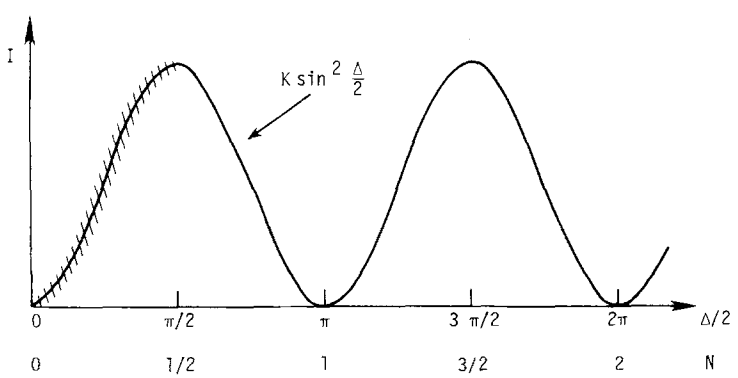

Fig. 2—Plot of radiation intensity

the intensities are read for a scan along this line. The light intensities are displayed on the screen as shown in Fig. 3.

The permissible operating range for HFP is from the minimum value (zero-order fringe) to the maximum value (half-order fringe). These two intensities are selected and their digitized Z values, as read by the system, are entered into the computer. The system will now record the Z values of all pixels in the field with 8-bit resolution (256 levels) within the range that was just selected. Intensities that are either higher or lower than the selected range will not be scaled.

It is immediately clear that the system does not have to operate from 'black' to 'white.' Within any field, any two points can be selected as maximum and minimum and the range between them will, within limits, be digitized to the same 8-bit resolution. Thus, once calibrated, the system can operate almost like a zoom microscope with respect to stress resolution. This feature, combined with a macro lens, yields a system that can at once do the overall analysis of a large stress field and then zoom into a small area with increased spatial (optical) and stress resolution. When operated through a microscope, very small stress details can be observed.

The theoretical fringe-order distribution that corresponds to the intensities depicted in Fig. 3 is a straight line. The two distributions can be related by combining eqs (3) and (4a). Thus:

$$Z = \psi \left[I_0 \sin^2 \frac{\Delta}{2} \right]^{\gamma} \tag{6}$$

or

$$\Delta = 2 \text{ arc sin } [AZ^{1/2\gamma}] \tag{7}$$

where

$A = [\psi^{1/\gamma} I_0]^{-1/2}$ is a constant that depends on the intensity of the light source and the sensitivity curve of the vidicon system

Finally, then eq (5) becomes

$$(\sigma_1 - \sigma_2) = \frac{2}{Ch} \text{ arc sin } [AZ^{1/2\gamma}] \tag{8a}$$

$$= \frac{f_\sigma}{\pi h} \text{ arc sin } [AZ^{1/2\gamma}] \tag{8b}$$

From eqs (1b) and (7) the partial fringe order

$$N = \frac{\Delta}{2\pi} = \frac{1}{\pi} \text{ arc sin } [AZ^{1/2\gamma}] \tag{9}$$

The values for A and γ can be obtained from eq (9) by measuring the actual partial fringe order (N) and the digitized intensity, or gray level (Z), for any two points in the optical field. This is best done with Tardy compensation.[5]

If the analyzer is mounted in a rotating stage with micrometer adjustment, the EYECOM system is unequaled in the accuracy with which it can perform Tardy compensations.

First, the plane polariscope must be rotated so that the isoclinic passes through the cursor location. This is very accurately done by requesting that the numeric value of the intensity at the desired point (pixel) can be displayed on the screen and then rotating the polariscope for a minimum value.

The quarter-wave plates are then reintroduced and the system is asked for an intensity scan along a short line transverse to the fringe direction at the point where compensation is required. The analyzer is rotated until the minimum intensity occurs at the point. This condition is shown in Fig. 4. The plot is for the intensities across the fringe at the cursor location over the length of the horizontal baseline. The system currently in use does not have a micrometer stage adjustment, yet it is possible to read the analyzer confidently to within 0.003 fringe, which is one order of magnitude better than when using the human eye for low-fringe order in the traditional way. The resultant plot, as shown in Fig. 4, can be greatly improved by using the averaging procedure described below.

The primary image, as displayed, is contaminated with optical and electrical noise. The former includes im-

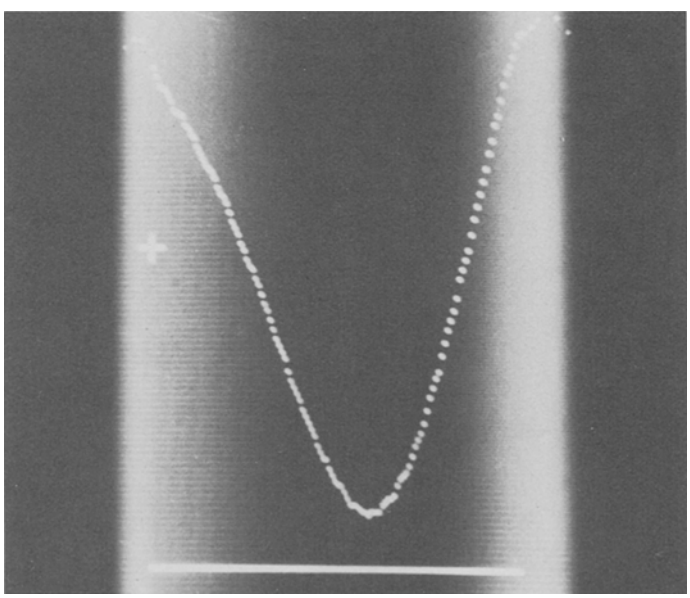

Fig. 3—Light intensities of the photoelastic response of a beam in bending

perfections of the light source, polariscope elements, lenses, and the model. The time varying random noise caused by electronics is dramatically reduced by scanning a number (16 in our operation) of consecutive pictures of the same photoelastic field and averaging the results. The operation is performed with built-in hardware functions.

Figure 5 presents the results of the calibration for a glass beam in pure bending. The positions across the beam are expressed in terms of the pixel number. Thus the total scan covered approximately 80 pixels on the video screen. As expected the data points for light intensity are nonlinear. The fringe orders at the same positions

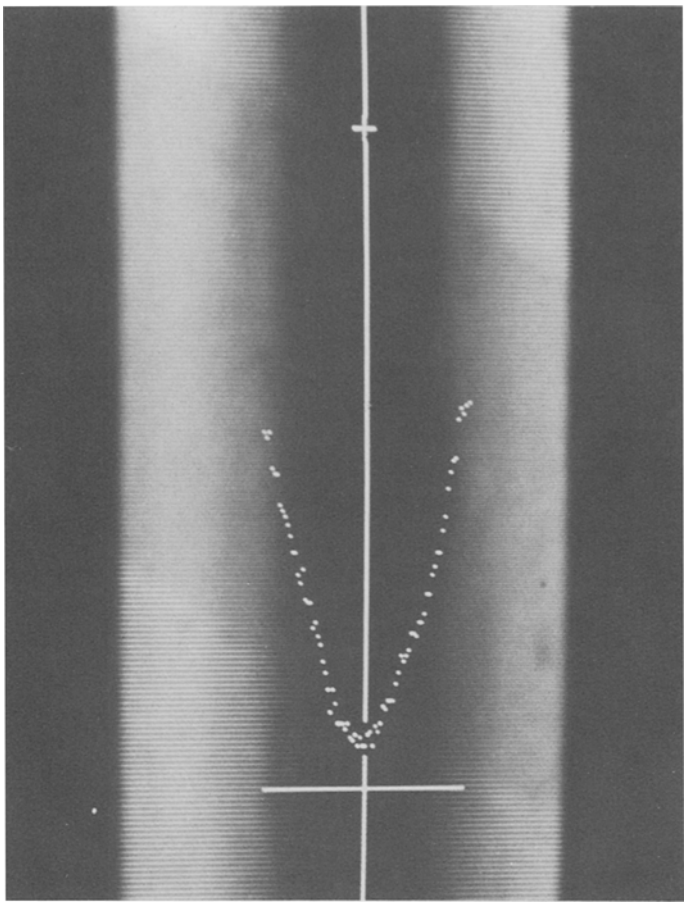

Fig. 4—Calibration of the HFP system with Tardy compensation

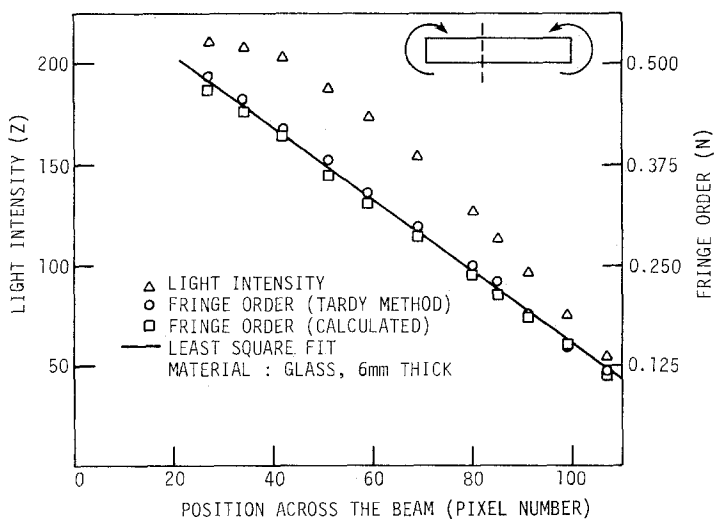

Fig. 5—Calibration plot of measured and calculated fringe orders

across the beam from Tardy compensation lie approximately along a straight line. Entering the data for each pair of points (N and Z) into eq (9), and solving in a least-square sense yields values for A and γ. If these values are used to calculate the fringe orders from the measured light intensities at each point, the results are the square data points on Fig. 5. The continuous line represents the best fit through all fringe-order points. The uncertainty in this method is less than 0.003 parts of the full-fringe order vs. 0.05 of the fringe order, when using the human eye to decide when the minimum intensity comes to the point.

The differences between calculated and measured fringe orders were within 3.5 percent.

Examples of Application of the HFP System

Concentrated Load on a Semi-infinite Plate

To demonstrate its use on materials with low-stress birefringence, the half-fringe-photoelasticity technique was applied to the problem of a concentrated load on the

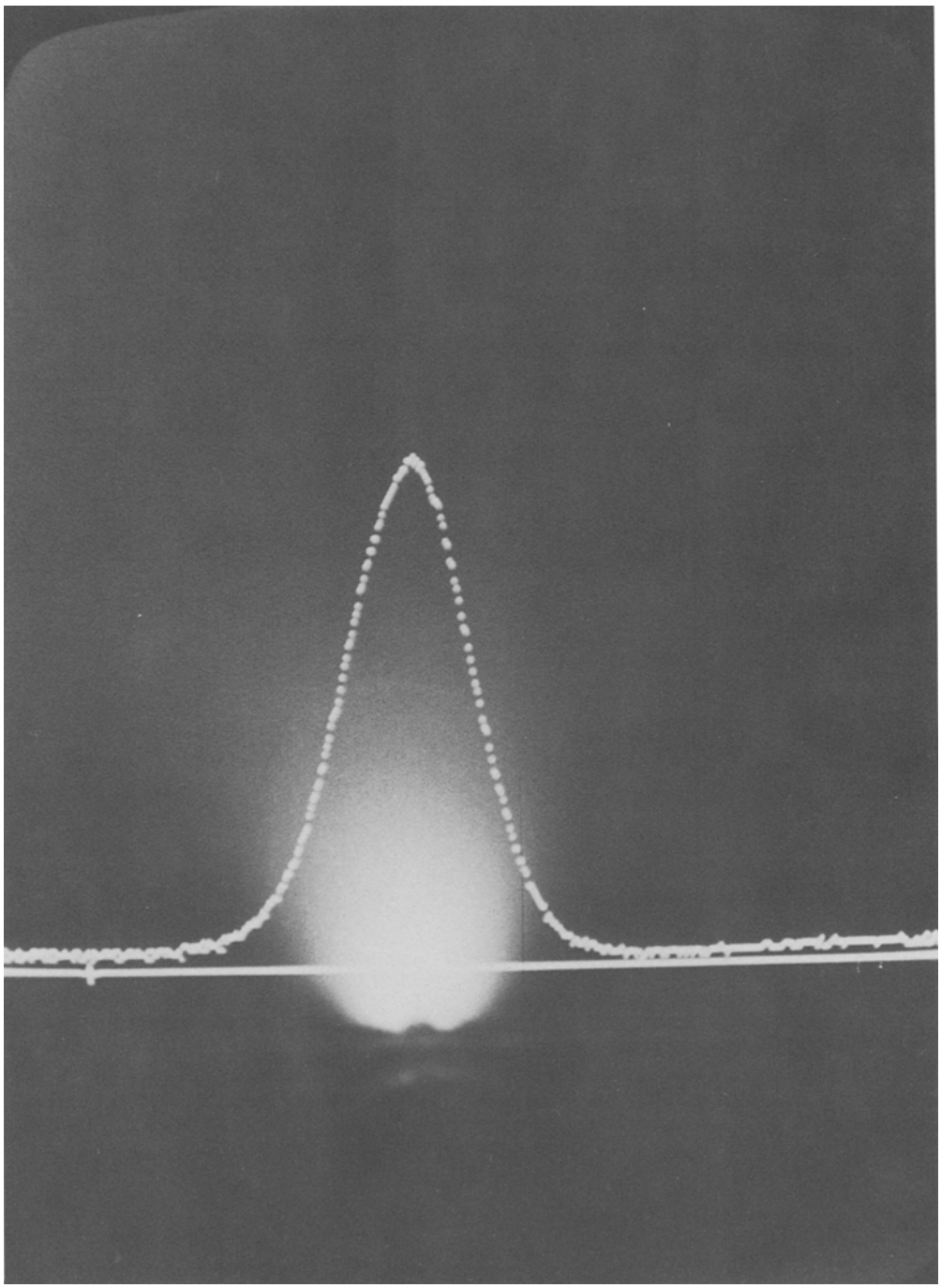

Fig. 6—Light-intensity plot for glass plate under concentrated load

edge of a semi-infinite glass plate. The edge of a glass model, $0.15 \times 0.15 \times 0.006$ m, was loaded with a concentrated load through a steel cylinder. The resultant optical response was observed through a transmission polariscope in the field of the video analyzer. After averaging the images from 16 scans to eliminate random noise, the picture was digitized and stored in the refresh memory. From here it could be recalled, viewed on the display monitor, and accessed by the computer for processing. An example of the photoelastic response for a particular load is shown in Fig. 6. The photograph shows the plot of intensities along an arbitrary section indicated by the continuous horizontal line. Each intensity can be related to fringe order (N) and stress ($\sigma_1 - \sigma_2$) by eqs (9) and (8) and the experimentally determined values of A and γ. To improve the visualization of the acquired information, artificial contouring was achieved by assigning partitions at specified intensity values (Fig. 7). Examination of this figure reveals that the loading force was inclined to the free surface. This procedure illustrates another important feature of the HFP technique's high level of resolution—the ability to evaluate the symmetry of loading by simple observation.

The measured intensities for the whole field were then converted to corresponding fringe values according to eq (9) and compared[4] to the results of a linear-elastic

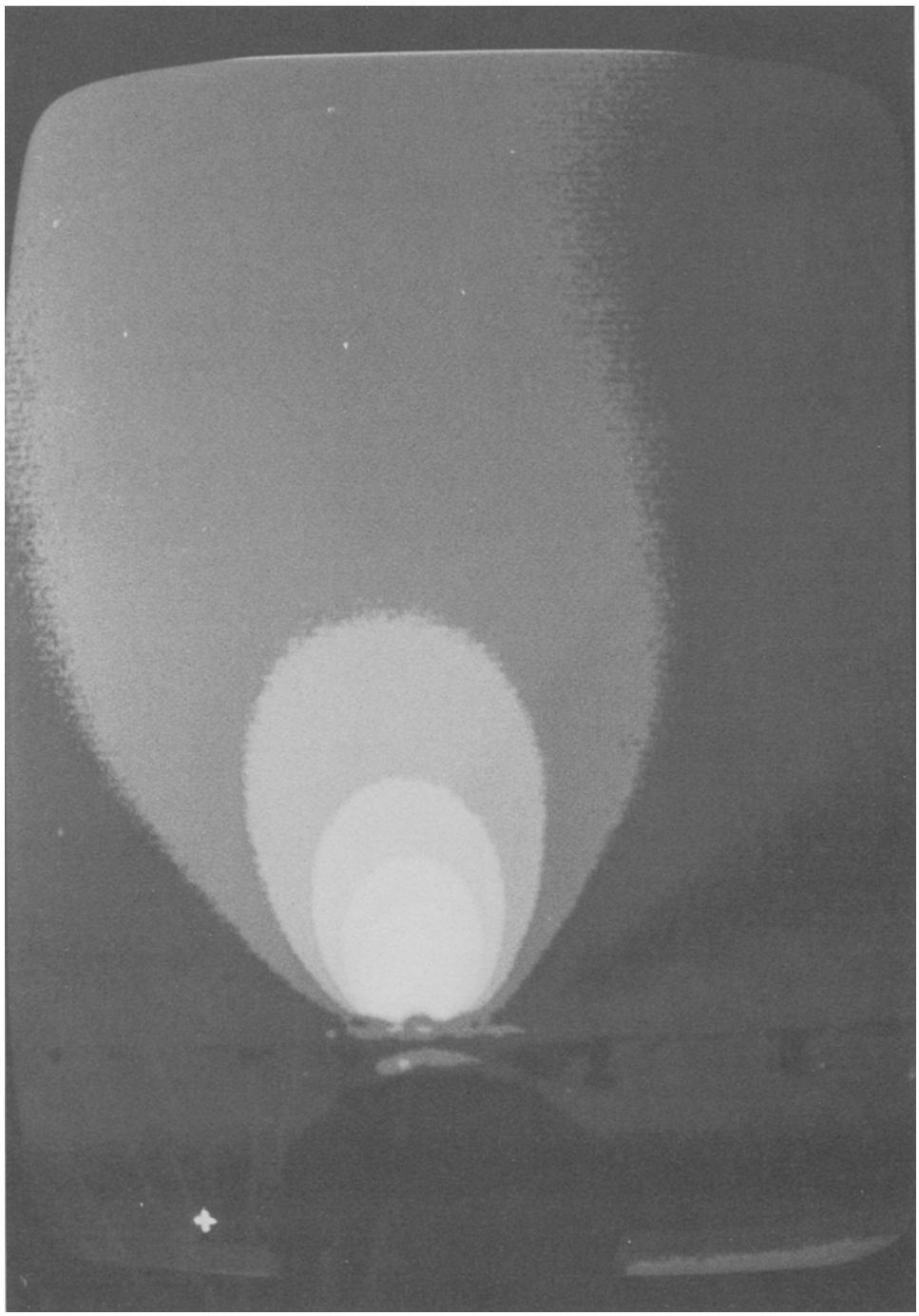

Fig. 7—Visualization of the acquired information by contouring with eight partitions

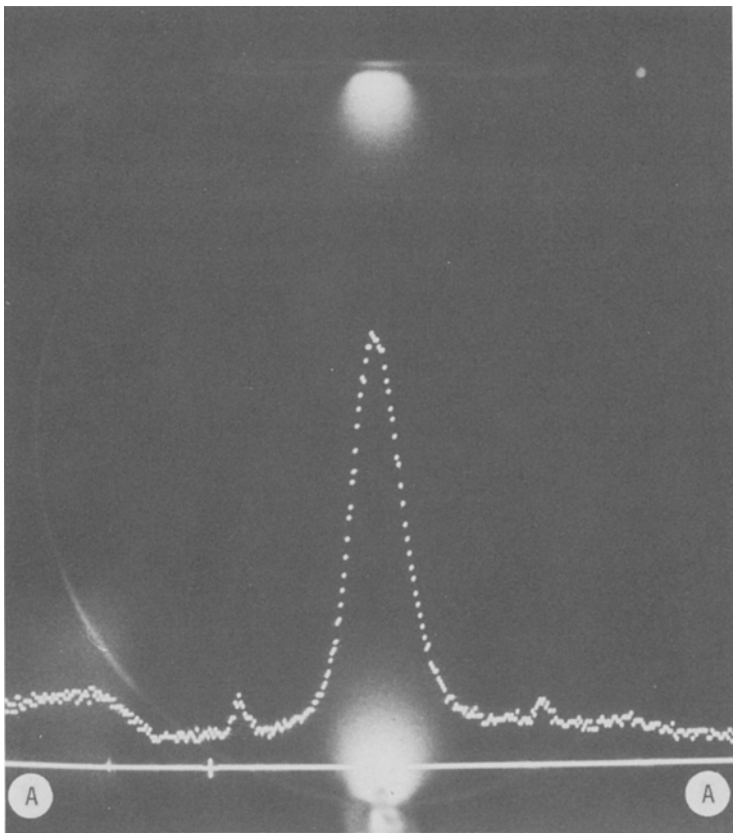

(a)

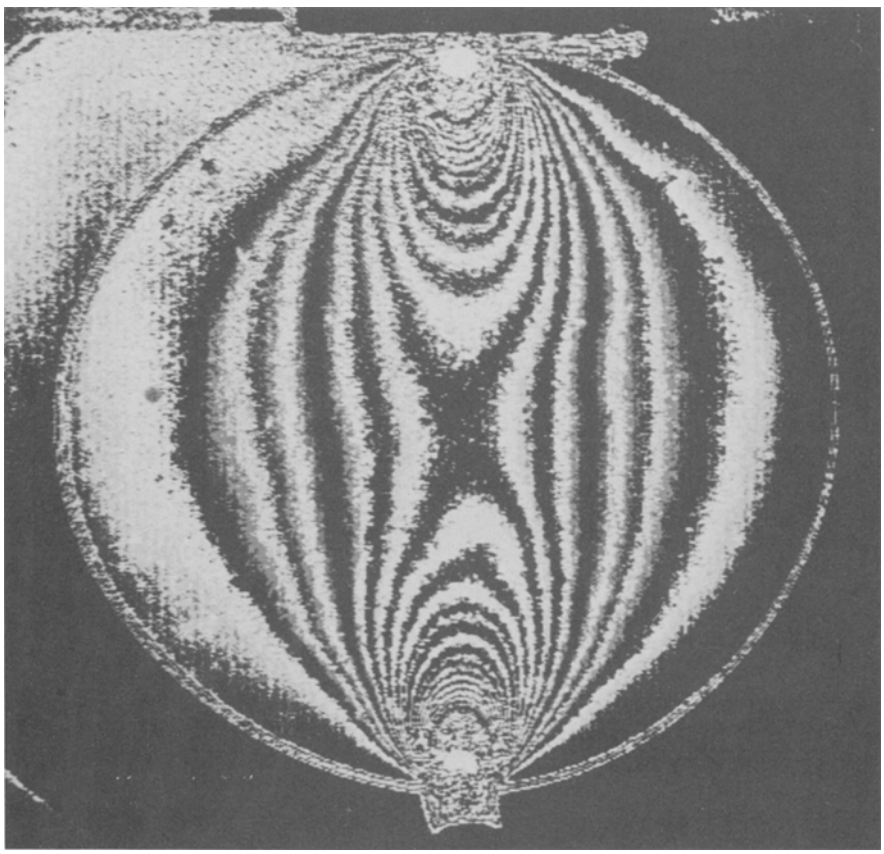

(b)

Fig. 8—Glass disk under diametral compression: (a) superimposed with light-intensity plot across AA, (b) visualization of the acquired light-intensity information

analysis.[6] The photoelastic and theoretical results were in good agreement.

Concentrated Diametral Loads on a Glass Disk

The case of the glass disk under diametral compression was used to illustrate a variation on the previous procedure. A glass disk, 65-mm in diameter and 3-mm thick, was loaded in diametral compression, so that approximately one half-fringe order was obtained when viewed in the dark field of a circular transmission polariscope.

Figure 8(a) is a picture of the image that appeared on the video screen. Superimposed on the basic image is a plot of the measured light intensities along the white line across the bottom of the picture.

A built-in hardware procedure may be used to identify the least significant binary digit and to assign 'black' to a zero and 'white' to a one. The result is Fig. 8(b), which now represents fringe-like lines which extend through the pixels with the same least significant bits. This does not convey any direct stress information but serves as another useful and rapid technique for checking symmetry of loading, stress gradients, and stress concentrations. Compare the clarity of this information with the diffuse nature of the original field, as shown in Fig. 8(a).

The calibration procedure provided a one-to-one correspondence between light intensity and partial fringe order. The conversion from light intensity to fringe order was made on the basis of eq (9), and the resulting contour map of equal fringe order is shown in Fig. 9(a). This unimproved picture depicts every 1/20th of a fringe (relative retardation 0.05 wavelength). For comparison, Fig. 9(b) shows the fringe pattern as calculated from the theoretical solution of a disk under diametral compression.[6]

Conclusions

The simple examples shown here illustrate the ability of contemporary digital image-analysis procedures for extracting high resolution photoelastic data from models with low levels of birefringence. It needs to be stressed that in these examples no digital filtering or image enhancement was performed. Only the time-varying electrical noise was removed by averaging the intensities recorded for 16 consecutive pictures.

This paper illustrates three of the major changes in normal photoelastic procedure:

(1) A glass model was used to study an elastic stress field with a resolution as good as or better than what could have been achieved with a polymeric model.

(2) Because a high-modulus glass model was used, the nonlinear behavior of the polymer in the highly stressed contact region was overcome. Under these high unit loads, polymers creep excessively—both in strain and

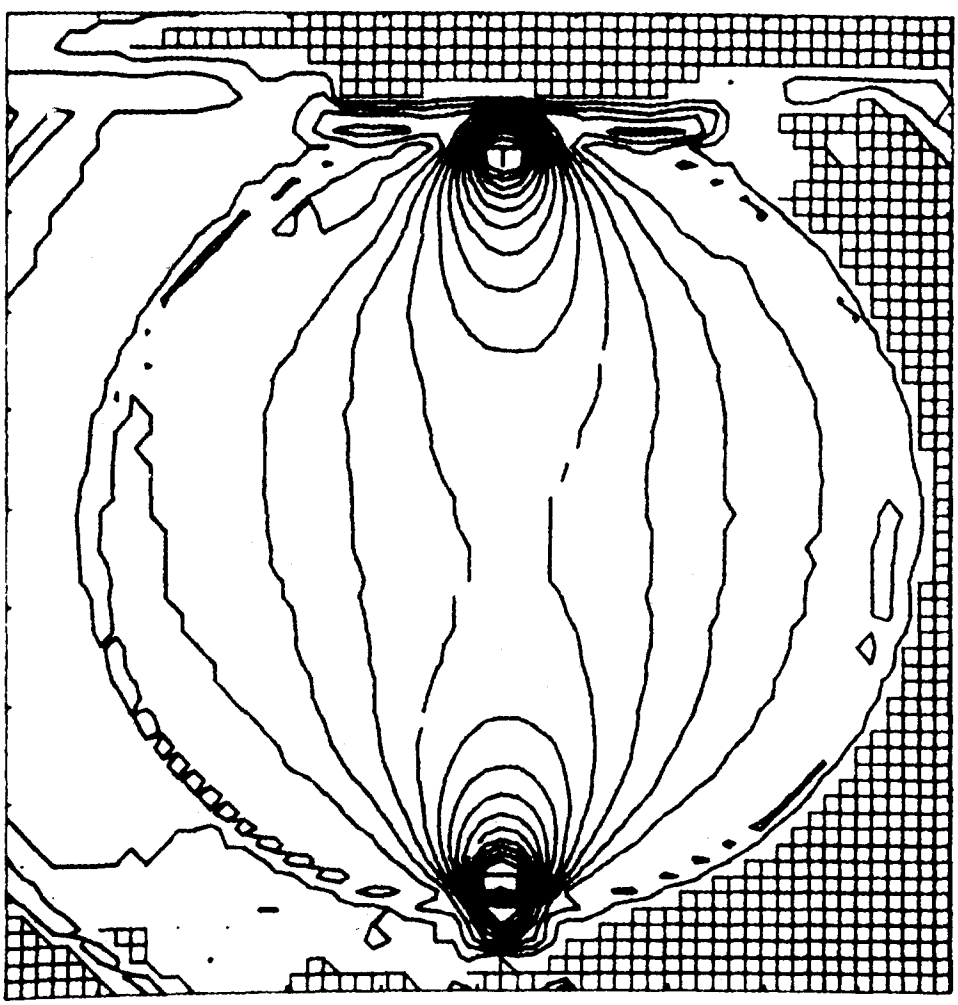

Fig. 9(a)—Contour map of equal fringe orders calculated from measured light intensities

fringe order. Consequently, the contact zone is larger than in typical structural materials under similar loads. Thus, the problem of large deformations is overcome.

(3) A full-field, fully automated photoelastic procedure was established.

By using these procedures many of the inherent difficulties of photoelasticity, which have precluded its use in the solution of many types of problems, can be overcome. Models can be made from materials that have been chosen for their ability to simulate prototype behavior. New and hitherto untried materials are available for use. Birefringent coatings can be thinner and many less transparent materials may become useful.

Some preliminary work shows the usefulness of the described method not just for isotropic materials, but also for composites which exert low levels of birefringence.[7] The high resolution of the system has been utilized in order to calculate stress-intensity factors under very low loads and to insure linear-elastic behavior near the tip of a crack.[8]

While this paper reports the preliminary results for this new approach to photoelasticity, it is already clear that the speed, efficiency, and resolution of the half-fringe-photoelasticity technique will place it in the forefront of future developments in experimental stress analysis.

Acknowledgments

This research was funded through NSF Grant CME 80 14066. The encouragement of Clifford Astill of the National Science Foundation and the support of both the Department of Engineering Science and Mechanics and the Engineering Research Institute at Iowa State University is gratefully acknowledged.

References

1. Zandman, F., "Photostress Analysis," Product Engineering, **30** *(9), 43-46 (March 2, 1959).*

2. Redner, S., "New Automatic Polariscope System," EXPERIMENTAL MECHANICS, **14** *(12), 486-491 (1974).*

3. Mueller, R.K. and Saackel, L., "Complete Automatic Analysis of Photoelastic fringes," EXPERIMENTAL MECHANICS, **19** *(7), 245-251 (1979).*

4. Burger, C.P. and Voloshin, A.S., "Half-fringe Photoelasticity: A New Instrument for Whole Field Stress Analysis," ISA Transactions, **22** *(2), 85-95 (1983).*

5. Kuske, A. and Robertson, G., Photoelastic Stress Analysis, John Wiley and Sons, London, 100-102 and 112 (1974).

6. Frocht, M.N., Photoelasticity, John Wiley and Sons, New York, **2**, *238 (1948).*

7. Voloshin, A.S. and Burger, C.P., "Photo-Orthotropic Elasticity Through a Digital Image Analysis of Low Level Bi-refringence," Proc. 7th Inter. Conf. on Exper. Stress Anal., Haifa, Israel, 483-494 (1982).

8. Miskioglu, I., Voloshin, A.S. and Burger, C.P., "Evaluation of Stress Intensity Factors Using Half-Fringe Photoelasticity," Abstracts 19th Annual Meeting Soc. of Eng. Sci., Rolla, MO, 100 (1982).

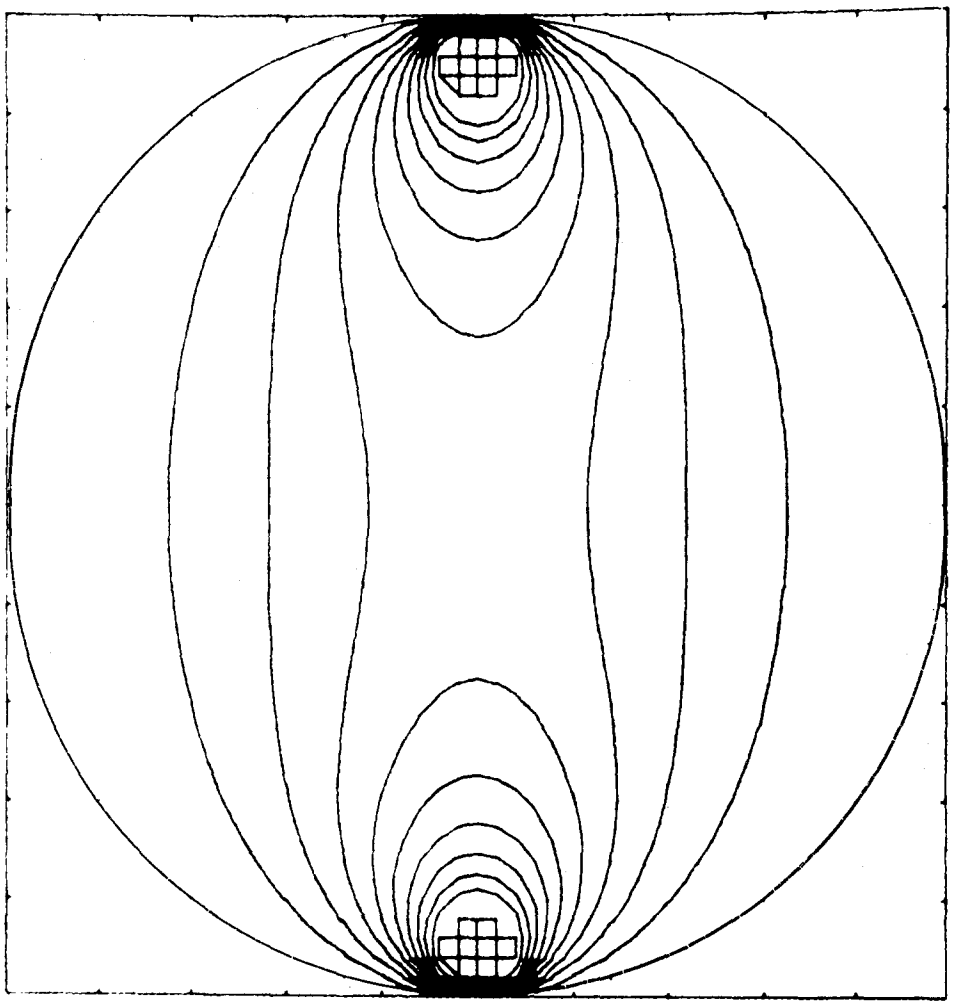

Fig. 9(b)—Contour map of equal fringe orders calculated from the theory